

## MODES ON A CONDUCTOR-BACKED SLOTLINE

**J. Machac, V. Kotlan, and M. Snajdr**

Czech Technical University in Prague  
Technicka 2, 16627 Prague 6, Czech Republic

**Abstract**—This paper reports on an experimental investigation of modes propagating along a conductor-backed slotline: the dominant mode, and the surface leaky mode. The measurement and the numerical experiments performed in the CST Microwave Studio verify theoretical findings of modes obtained by the method of moments applied in the spectral domain. The dispersion characteristic of the dominant mode on the conductor-backed slotline is determined by substituting this line by a flat slotted waveguide.

### 1. INTRODUCTION

Planar and uniplanar transmission lines have become basic building blocks of MIC and MMIC circuits. Among these lines, the conductor-backed slotline and the conductor-backed CPW are of marginal interest for designers, as there is always some power leakage into the substrate. Additional measures have been applied to prevent power leakage from these lines, e.g., dividing the substrate into two layers, using a superstrate, or confining the line laterally by conducting vias [1–3]. Elsewhere, the conductor-backed slotline has been applied as a leaky wave antenna [4], making use of space leaky wave excitation. Restricting the conductor-backed slotline substrate on the sides by conducting walls, we obtain a flat slotted waveguide [5]. The cross sections of these lines are shown in Fig. 1. Here, we analyze a lossless, laterally and longitudinally unbounded conductor-backed slotline.

We have presented a dominant mode of the conductor-backed slotline [6–8]. This mode can propagate along this line from zero frequency, and is not a bound mode [6], the propagation constant of this mode is, however, real. The distribution of its field in the substrate between the metal plates forms in the transversal direction a standing wave, see Fig. 2. We have proved the presence of this mode experimentally [7, 8] on a finite sized conductor-backed slotline with a

substrate 6 mm in thickness with permittivity 2.6. Our original finding was that the phase constant of this mode on a line with a sufficiently wide slot decreases below the free space propagation constant. There is even a frequency band in which no solution of the dispersion equation was found for this mode [7]. This paper presents the results of careful measurement verifying the behavior of this mode.

We have revealed the peculiar behavior of a surface leaky mode of the first order on the conductor-backed slotline in dependence on the slot width [7]. Its dispersion characteristic has two branches starting from a certain slot width. This characteristic is an ambiguous function of frequency. The originally nonphysical upper branch becomes physical if the slot is further widened. The two corresponding surface leaky modes are excited simultaneously. Careful measurement of the electric field distribution along the front edge of the conductor-backed slotline substrate verified this behavior experimentally.

In this paper we will concentrate on modes with even symmetry of the transversal component of the electric field directed across the slot, as these modes can be simply excited by a source connected across the slot, e.g., a coaxial cable. The results of measurement were verified by the CST Microwave Studio professional code.

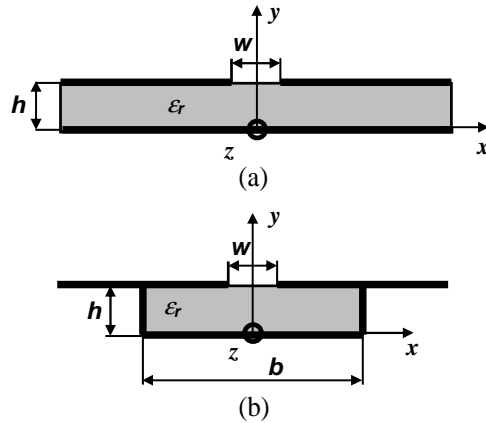


**Figure 1.** Cross section of the conductor-backed slotline (a), and the flat slotted waveguide (b).

An improved APTL code analyzing planar transmission lines [9] based on the method of moments applied in the spectral domain, explained, e.g., in [10], were used to calculate the mode propagation constants and the field distributions. This code calculates complex propagation constants and transversal field distributions of all possible

modes (bound, surface, and space leaky) propagating on 24 various kind of planar transmissions lines. The validity of the APTL code results was many times successfully tested for various planar lines. The conductor-backed slotline was analyzed by the authors in [6], where the computed complex propagation constant was compared with the only relevant data published for the conductor-backed slotline in [11, 12]. This constant was calculated by the mode matching method applied to the conductor-backed slotline in [11]. A line on the substrate with permittivity 2.25 had the top cover  $12.5h$  from the upper line surface. According to [11] the height of the cover plate has a minor influence on the propagation constant. The same line, but without the top shielding was analyzed using the spectral domain method in [12]. The comparison of the obtained data was done in Fig. 2 of [6]. The shapes of the dispersion characteristics resemble each other well. Consequently the APTL code can be considered sound and reliable.

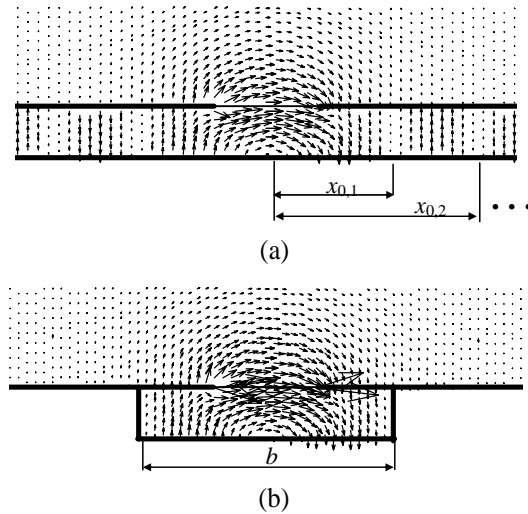


**Figure 2.** Calculated electric field distribution of the dominant mode on the conductor-backed slotline (a), and of the bound mode on the flat slotted waveguide  $b = 2x_0$  in width (b). The normalized frequency is  $h/\lambda_0 = 0.25$ . The line parameters are  $w = 12$  mm,  $h = 6$  mm,  $\varepsilon_r = 2.6$ , the zero field point position is  $x_0 = 14,757$  mm, so  $b = 29.514$  mm.

## 2. DOMINANT MODE ON A CONDUCTOR-BACKED SLOTLINE

Propagation of the dominant mode on the conductor-backed slotline is modeled by substituting this line by a flat slotted waveguide. The conducting sidewalls of the slotted waveguide are located where the original dominant mode electric field component perpendicular to substrate walls is zero.

The calculated electric field of the dominant mode on the conductor-backed slotline is shown in Fig. 2(a) at the normalized frequency  $h/\lambda_0 = 0.25$ , where  $\lambda_0$  is the free space wavelength and  $h$  is substrate thickness. Fig. 2(b) shows the electric field of the bound mode on the flat slotted waveguide at the same frequency with the same line parameters: slot width  $w = 12$  mm, substrate thickness  $h = 6$  mm,

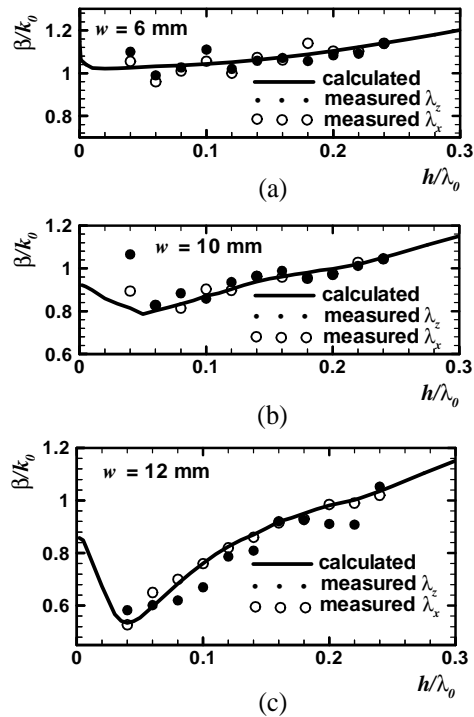


**Figure 3.** Calculated and measured normalized dispersion characteristics of the dominant mode on the lines with  $h = 6$  mm, permittivity 2.6 and different  $w$ . The way of obtaining the experimental results is described in paragraph 4.1.

and permittivity  $\varepsilon_r = 2.6$ . The width of the flat slotted waveguide equals double the first zero field point from Fig. 2(a),  $b = 2x_0$ . The field distributions in Figs. 2(a) and (b) are identical within the volume limited by  $x_0$ . The field distributions in Fig. 2 have even symmetry with respect to the  $E_x$  field component. This symmetry corresponds to the symmetry of electric wall located in the  $yz$  plane, as expected for slotline modes. Violation of symmetry at the slot edges is due to numerical errors. Fig. 3 shows the normalized phase constant  $\beta/k_0$  of the dominant mode on the conductor-backed slotline calculated by the APTL code for different slot widths.  $k_0$  is the free space wavenumber. The phase constant is determined iteratively. By estimating the phase constant of the dominant mode of the conductor-backed slotline we determine the first zero field point. We thus define the flat slotted waveguide width and we calculate the phase constant of the flat slotted waveguide mode. This value is used as the starting point for recalculating the conductor-backed slotline dominant mode phase constant. This process is repeated until the difference between the phase constants of the modes on the conductor-backed slotline and the flat slotted waveguide is sufficiently small.

### 3. SURFACE LEAKY MODE ON CONDUCTOR-BACKED SLOTLINE

The dispersion characteristic of the surface leaky mode evolves gradually, in a peculiar manner, with increasing slot width  $w$ . For a narrow slot, Fig. 4, we have one complex physical solution of the dispersion equation representing the surface leaky mode and one complex nonphysical solution with the phase constant greater than  $k_{TEM} = \sqrt{\varepsilon_r}k_0$ , the phase constant of the substrate TEM mode.  $\alpha/k_0$  is the normalized attenuation constant. These two complex solutions split from a real nonphysical solution of the dispersion equation at two separate points, see Fig. 4. Increasing the slot width, these two splitting points come closer together and, finally, at around  $w = 7$  mm they merge and the two complex solutions of the dispersion equation corresponding to the leaky waves create a single dispersion characteristic with two branches. The phase constant of the originally nonphysical solution, which was greater than  $k_{TEM}$ , decreases with increasing  $w$  and finally the corresponding mode becomes physical. This is documented in Fig. 5, where the dispersion characteristics of the conductor-backed slotline are plotted as in Fig. 4, but now for  $w = 10$  mm.

Further widening of the slot modifies the dispersion characteristics of the surface leaky wave. This is shown in Fig. 6, where the

characteristics are plotted for  $w$  equal to 13, 13.2, 13.5 and 14 mm. At  $w = 13.2$  mm the two branches of the dispersion characteristic are still connected, but from  $w = 13.5$  mm upwards they are disconnected into two separate branches.

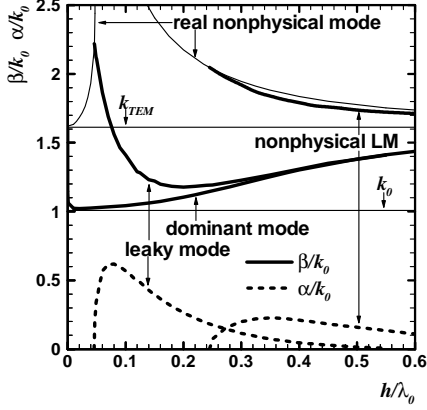


**Figure 4.** Calculated normalized dispersion characteristics of the even dominant and even leaky modes on the conductor-backed slotline with  $w = 6$  mm,  $h = 6$  mm, and  $\varepsilon_r = 2.6$ .

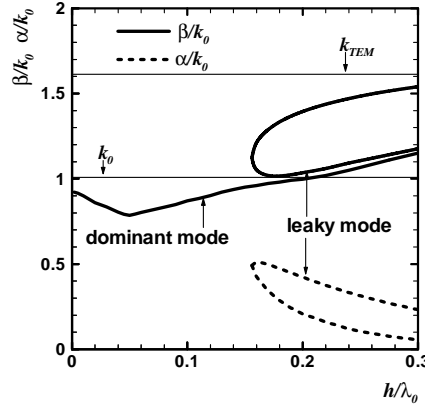


**Figure 5.** Calculated normalized dispersion characteristics of the even dominant and even leaky modes on the conductor-backed slotline with  $w = 10$  mm,  $h = 6$  mm, and  $\varepsilon_r = 2.6$ .

#### 4. EXPERIMENT, NUMERICAL EXPERIMENT

The experimentally investigated conductor-backed slotline was on a plexiglass substrate with 2.6 permittivity and 6 mm in thickness. The substrate was 2 m in width and 1.5 m in length. We measured the electric field along the slot of the conductor-backed slotline and transversally to its axis along the front edge of the substrate. The electric field was measured by a coaxial probe driven mechanically by a step motor, and controlled by a computer [13]. The measured field distributions are distorted by the manifold internal reflections of the field within the interior of the substrate. Thus, in some cases of measured distributions, it is difficult to recognize the expected character of the field. The measurement was performed in the frequency range from 2 up to 12 GHz, which, for a substrate 6 mm in thickness, corresponds to the range of normalized frequencies  $h/\lambda_0$  from 0.04 up to 0.24. The propagation constants and the leakage angles

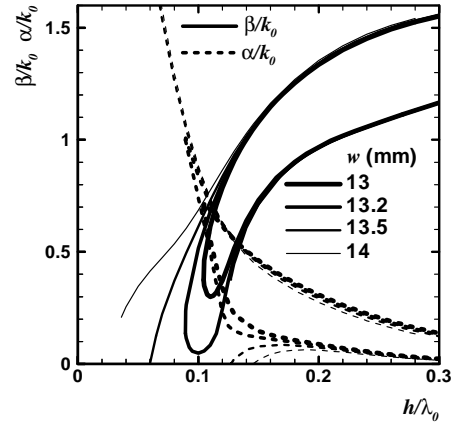


**Figure 6.** Calculated normalized dispersion characteristics of the even leaky mode on the conductor-backed slotline with  $h = 6$  mm, and  $\epsilon_r = 2.6$  for different  $w$ .

calculated from measured field distributions were compared with data computed by the APTL code [9] and with the results of numerical simulations performed in the CST Microwave Studio. The modes with even distribution of field  $E_x$  were investigated. To excite these modes, the slotline was fed via a coaxial line, as shown in Fig. 7. Unfortunately, this feeding circuit is not symmetrical. It therefore excites the field in the substrate non-symmetrically. This has been proved by a simulation performed in the CST Microwave Studio, Fig. 8, and also by measurement. There is a distribution that more adequately reflects the theoretically predicted results on the side where the central conductor of the coaxial line is connected. The field distributions measured on this side were therefore used to determine the propagation constants presented in the following text.

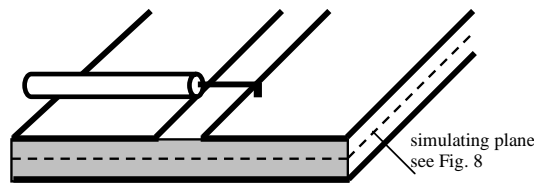


**Figure 7.** The feeding circuit.

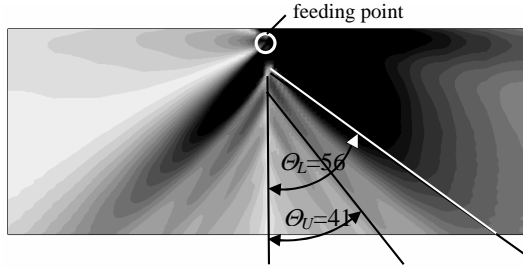


**Figure 8.** The  $E_y$  field distribution calculated by the CST Microwave Studio at the central level  $y = 3$  mm of the substrate of the conductor-backed slotline with  $w = 12$  mm at the normalized frequency 0.18. The conductor-backed slotline is fed through the coaxial line from the left, as shown in Fig. 7.

#### 4.1. Dominant Mode

The phase constant of the dominant mode was determined in two ways. First, the standing wave pattern of field  $E_x$  was measured along the line. The mode phase constant is directly calculated from the wavelength. The second way follows from the standing wave character of the field of the dominant mode in the substrate between the conducting planes, as shown in Fig. 2(a). We take the distribution of  $E_y$  along the front edge of the substrate transversal to the slot. An example of this distribution for a slot 12 mm in width is shown in Fig. 9, measured at the normalized frequency  $h/\lambda_0 = 0.24$ . The line was fed at a distance 300 mm from the edge of the substrate. The

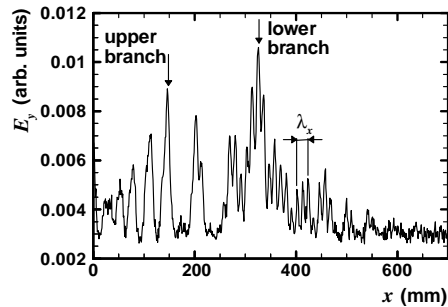


**Figure 9.** Distribution of the electric field measured along the edge of the substrate at the normalized frequency  $h/\lambda_0 = 0.24$ , i.e., 12 GHz for the used substrate. The line with  $w = 12$  mm,  $h = 6$  mm,  $\epsilon_r = 2.6$ .



standing wave pattern of the dominant mode corresponds to the fine quasi-periodic structure of the measured field distribution [8] apparent at a range of coordinate  $x$  from 250 to 500 mm, Fig. 9 where wavelength  $\lambda_x$  is figured. Its wavelength determines the propagation constant in the  $x$ -direction  $\beta_x$ , and, consequently, the dominant mode longitudinal propagation constant is [14]

$$\beta = \sqrt{k_{TEM}^2 - \beta_x^2}. \quad (1)$$

The measured propagation constants of the dominant mode on the conductor-backed slotline with three different slot widths 6, 10, 12 mm are plotted together with the calculated propagation constant in Fig. 3. Here “measured  $\lambda_z$ ” marks the phase constant calculated using the standing wave pattern measurement along the slot, and “measured  $\lambda_x$ ” marks the propagation constant determined by (1) from the indirect field measurement taken along the slot edge. The differences between the phase constants measured by the two above presented ways can be attributed to field distorted in the volume of the substrate by internal reflections on its edges. But in spite of this the data shown in Fig. 3 fit together sufficiently well.

#### 4.2. Surface Leaky Mode

The surface leaky mode was experimentally verified as in the set-up used in [11]. The existence of the leaky mode has to be determined by twice measuring the distribution of field  $E_y$  along the front edge of the substrate perpendicular to the slot, basically at two different distances of the coaxial feeder from the front edge. Leakage angle  $\Theta$  is then determined from the positions of the two corresponding maxima of the field in these plots. This eliminates the error caused by the different position of the feeder from the phase center of the excited surface leaky mode revealed in the field distributions calculated by the CST Microwave Studio, Fig. 8. The leaky mode phase constant can be determined from the known leakage angle only if we neglect the mode attenuation constant and the losses of the conductor-backed slotline itself [14]. In this case

$$\beta = k_{TEM} \cos \Theta. \quad (2)$$

Taking into account leaky mode complex propagation constant  $\gamma = \beta - j\alpha$  we have

$$\Theta = \arctan \left( \frac{\xi_{pr}}{\beta} \right), \quad (3)$$

where  $\xi_{pr}$  is the real part of the position of the pole of the Green function used in the method of moments expressed in the spectral domain [14]. The problem of applying (3) to determine the phase constant is that we do not know from the experiment the quantities that are needed to determine  $\xi_{pr}$ . In the following text we will therefore compare only the leakage angles determined from the measured field distributions with the leakage angles calculated from the output of the APTL code using (2) and (3), and angles read from the results of simulations done in the CST Microwave Studio. The two angles determined by (2) and (3) are different due to the nonzero value of the attenuation constant [14]. They serve as two limits for the measured data.

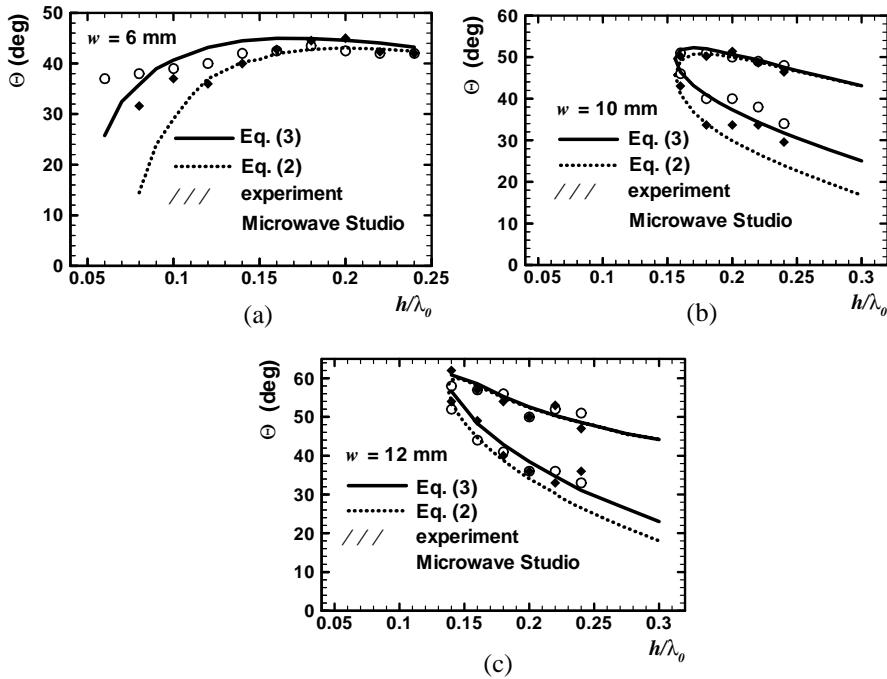


**Figure 10.** Measured and calculated leakage angles of the surface leaky mode on the lines with  $h = 6$  mm, permittivity 2.6, and different  $w$ .

The distribution of the electric field along the edge of the substrate was measured for three different positions of the coaxial feeder distant 300 mm, 440 mm, and 550 mm from this edge, in order to provide more data for determining the leakage angles. An example of the measured

field distribution is shown in Fig. 9. The two maxima of the field correspond to the two leaky modes. For the upper branch of the dispersion characteristic the maximum is at  $x = 150$  mm, and for the lower branch the maximum is at  $x = 325$  mm. Fig. 10 shows the leakage angles recalculated by (2) and (3) from the dispersion characteristics calculated by the APTL code, and plotted for  $w = 6$  and 10 mm in Figs. 4 and 5. At  $w = 6$  mm we have, Fig. 4, one branch of the dispersion characteristic, whereas at  $w = 10$  mm and greater we have two branches. Fig. 10 shows certain discrepancies between the measured, simulated and calculated data. The reasons are again as in the case of the dominant mode in the field distorted by internal reflections at the substrate edges and in the fact that we cannot read precisely the leakage angles from the field distributions calculated by the CST Microwave Studio.

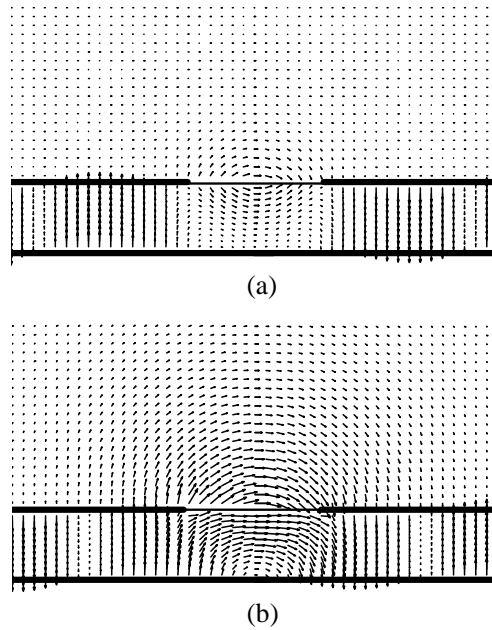


**Figure 11.** The imaginary part of the electric field distribution in the transversal plane of the conductor-backed slotline with a slot 12 mm in width calculated by the APTL code at  $h/\lambda_0 = 0.18$  for the surface leaky mode with higher phase constant  $\beta/k_0 = 1.252$  (a), and with lower phase constant  $\beta/k_0 = 0.923$  (b).

The existence of the two branches of the surface leaky mode dispersion characteristics was additionally verified by a numerical

experiment performed in the CST Microwave Studio. The conductor-backed slotline structure in this case has a substrate 800 mm in width and 350 mm in length terminated by “open” boundaries to model the infinite structure. The conductor-backed slotline is fed via the coaxial line from the left, as shown in Fig. 7. The calculated distribution of field  $E_y$  plotted in Fig. 8, taken for the conductor-backed slotline with a slot 12 mm in width, and at normalized frequency 0.18, shows the two maxima directed from the slot at the leaky angles  $\Theta_L = 56^\circ$ ,  $\Theta_U = 41^\circ$ . The more intensive maximum represents the mode that corresponds to the lower branch of the dispersion characteristic.

Through experiments and in the CST Microwave Studio it is not possible to distinguish the fields originating from the two particular modes. They can be distinguished only by using the APTL code. The results show that the field distributions in the transversal plane of the two modes corresponding to the two branches of the dispersion characteristic are different. The leaky mode, the propagation constant of which corresponds to the upper branch of the dispersion characteristic, has a higher attenuation constant. Its field therefore increases more rapidly in the transversal direction than the field of the mode with a lower phase constant, as shown in Fig. 11. The field of this latter mode is more tightly confined to the vicinity of the slot, Fig. 11.

## 5. CONCLUSION

This paper reports on an investigation of the conductor-backed slotline, and namely modes with even symmetry of the transversal electric field component.

The dispersion characteristics of the dominant mode on the conductor-backed slotline have been presented. These characteristics were calculated by substituting the conductor-backed slotline by a flat slotted waveguide. The width of this waveguide was set equal to double the first zero field point position of the dominant mode on the conductor-backed slotline.

The measurement confirmed the existence of the dominant mode and the even surface leaky mode on a conductor-backed slotline. The dominant mode propagates from zero frequency and it always accompanies the propagating surface leaky modes. The phase constant of this mode was determined using the wavelength taken from the standing wave pattern measured along the line, and additionally from the standing wave pattern of this mode measured along the front edge of the substrate. The measured phase constants fit the calculated values well, even in frequency ranges where theory has predicted that

the dominant mode phase constant will be lower than the free space propagation constant.

Above a certain slot width, the dispersion characteristic of the even surface leaky mode shows the ambiguous character of the function with two branches. The leaky modes corresponding to the two branches have different phase and attenuation constants and, therefore, different leakage angles. This was observed in the measured field distributions taken along the front edge of the substrate perpendicular to the slot. Due to this fact it was possible to detect these two modes. The field distribution of these two modes in the transversal plane differs, as shown by the results of the simulations done by the APTL code. The leakage angle of these modes was calculated both without and with a correction for the attenuation constant [14]. The measured angles are mostly somewhere in between these two values. We are not able from our measurements directly to determine the mode propagation constant, as we do not know the value of the attenuation constant and, consequently, the position of the complex pole. The existence of the two surface leaky modes on the conductor-backed slotline corresponding to the two branches of the dispersion characteristic was confirmed by a numerical simulation performed in the CST Microwave Studio.

## ACKNOWLEDGMENT

This work has been supported by the Grant Agency of the Czech Republic under project 102/06/1106 “Metamaterials, nanostructures and their applications”.

## REFERENCES

1. Liu, Y., K. Cha, and T. Itoh, “Non-leaky coplanar (NLC) waveguides with conductor backing,” *IEEE Trans. Microwave Theory and Tech.*, Vol. 43, No. 5, 1067–1072, May 1995.
2. Das, N. K., “Methods of suppression or avoidance of parallel-plate power leakage from conductor-backed transmission lines,” *IEEE Trans. Microwave Theory and Tech.*, Vol. 44, No. 2, 169–181, February 1996.
3. Haydl, W. H., “On the use of vias in conductor-backed coplanar circuits,” *IEEE Trans. Microwave Theory and Tech.*, Vol. 50, No. 6, 1571–1577, June 2002.
4. Machac, J., J. Zehentner, and J. Hruska, “Conductor-backed slotline antenna,” *Proceedings of the 34th European Microwave*

- Conference*, Vol. 2, 1205–1208, Amsterdam, Netherlands, October 2004.
5. Zehentner, J., J. Machac, and J. Mrkvica, “Flat waveguide with a longitudinal slot,” *2005 IEEE MTT-S International Microwave Symposium Digest*, TH4C-4, Long Beach, Ca., USA, June 2005.
  6. Zehentner, J., J. Machac, and J. Mrkvica, “Novel selected modes on the conductor-backed slotline,” *2002 IEEE MTT-S International Microwave Symposium Digest*, Vol. 2, 961–964, Seattle, Wash., USA, June 2002.
  7. Zehentner, J., J. Machac, and J. Mrkvica, “Even and odd modes on a conductor-backed slotline,” *Proceedings of the 32nd European Microwave Conference*, Vol. 3, 609–612, Milan, Italy, September 2002.
  8. Zehentner, J., J. Machac, J. Mrkvica, J. Hruska, V. Langer, and P. Zabloudil, “Experimental verification of theoretically revealed modes on the conductor-backed slotline,” *Proceedings of 2002 Asia-Pacific Microwave Conference*, Vol. 2, 1200–1203, Kyoto, Japan, November 2002.
  9. Zehentner, J., J. Mrkvica, and J. Machac, “Analysis and design of open planar transmission lines,” *East-West Workshop on Advanced Techniques in Electromagnetics*, Warszawa, Poland, May 2004.
  10. Zehentner, J., J. Macháč, and M. Migliozzi, “Upper cut-off frequency of the bound wave and new leaky wave on the slotline,” *IEEE Trans. Microwave Theory and Techn.*, Vol. 46, No. 4, 378–386, April 1998.
  11. Shigesawa, H., M. Tsuji, and A. A. Oliner, “Conductorbacked slot line and coplanar waveguide: Dangers and fullwave analysis,” *1988 IEEE MTT-S Int. Microwave Symp. Dig.*, Vol. 1, 199–202, June 1988.
  12. Das, N. K. and D. M. Pozar, “Full-wave spectral-domain computation of material, radiation, and guided wave losses in infinite multilayered printed transmission lines,” *IEEE Trans. Microwave Theory and Tech.*, Vol. 39, No. 1, 54–63, January 1991.
  13. Holubec, B., L. Jelinek, J. Machac, and J. Zehentner, “Computer controlled measurements of electromagnetic fields,” *Proceedings of the 16th International Czech-Slovak Scientific Conference Radioelektronika 2006*, 284–287, Bratislava, Slovakia, April 2006.
  14. Machac, J. and J. Zehentner, “Comments on representation of surface leaky waves on uniplanar transmission lines,” *IEEE Trans. Microwave Theory and Tech.*, Vol. 50, No. 2, 583–585, February 2002.